Published in final edited form as:
Biochemistry. 2011 October 25; 50(42): 9066–9075. doi:10.1021/bi201094v.

Substitution of the human αC region with the analogous chicken domain generates a fibrinogen with severely impaired lateral aggregation: fibrin monomers assemble into protofibrils but protofibrils do not assemble into fibers.†

Lifang Ping[#], **Lihong Huang**[#], **Barbara Cardinali**[#], **Aldo Profumo**[‡], **Oleg V. Gorkun**[#], and **Susan T. Lord**[#,*]

[#]Department of Pathology and Laboratory Medicine, University of North Carolina at Chapel Hill, Chapel Hill, NC 27599-7525, USA

[‡]Biopolimeri e Proteomica, Istituto Nazionale per la Ricerca sul Cancro (IST), Largo R. Benzi 10, Genoa, Italy

Abstract

Fibrin polymerization occurs in two steps: the assembly of fibrin monomers into protofibrils and the lateral aggregation of protofibrils into fibers. Here we describe a novel fibrinogen that apparently impairs only lateral aggregation. This variant is a hybrid, where the human αC region has been replaced with the homologous chicken region. Several experiments indicate this hybrid human-chicken (HC) fibrinogen has an overall structure similar to normal. Thrombin-catalyzed fibrinopeptide release from HC fibrinogen was normal. Plasmin digests of HC fibrinogen produced fragments that were similar to normal D and E; further, as with normal fibrinogen, the knob 'A' peptide, GPRP, reversed the plasmin cleavage associated with addition of EDTA. Dynamic light scattering and turbidity studies with HC fibrinogen showed polymerization was not normal. Whereas early small increases in hydrodynamic radius and absorbance paralleled the increases seen during the assembly of normal protofibrils, HC fibrinogen showed no dramatic increase in scattering as observed with normal lateral aggregation. To determine whether HC and normal fibrinogen could form a copolymer, we examined mixtures of these. Polymerization of normal fibrinogen was markedly changed by HC fibrinogen, as expected for mixed polymers. When the mixture contained 0.45 μM normal and 0.15 M HC fibrinogen, the initiation of lateral aggregation was delayed and the final fiber size was reduced relative to normal fibrinogen at 0.45 μM. Considered altogether our data suggest that HC fibrin monomers can assemble into protofibrils or protofibril-like structures but these either cannot assemble into fibers or assemble into very thin fibers.

During coagulation the soluble plasma glycoprotein fibrinogen is converted into fibrin fibers that serve as the insoluble scaffold support for blood clots. Fibrinogen is composed of six polypeptides, two copies each of three non-identical chains called Aα, Bβ, and γ. High-resolution crystallography data show these chains are assembled into a multi-nodular protein, with a unique central region and a pair of symmetric peripheral regions, linked by

†This work was supported by the National Institutes of Health (HL31048) and the National Science Foundation (0705977).

*Corresponding author: University of North Carolina at Chapel Hill Department of Pathology and Laboratory Medicine Chapel Hill, NC 27599-7525 Phone: 919 966 3548 Fax: 919 966 6718 stl@med.unc.edu.

Supporting Information Available

Figure S1 presents the peptide mass fingerprinting results of the two HC fibrinogen bands resolved on reduced SDS-PAGE. Peptide coverage and the identified peptides are shown. This material is available free of charge via the Internet at http://pubs.acs.org.

coiled-coil connectors (1). (We use the recommended nomenclature to describe fibrinogen and fibrin structure (2)). The central region contains the N-termini of all six chains and can be isolated from a plasmin digest of fibrinogen as the fragment called E. The C-termini of each set of three chains extend in opposite directions from the center, as a three chain coiled-coil. The Bβ- and γ-chains each terminate as independent globular nodules. These nodules are closely associated and can be isolated as the proteolytic fragment called D. The Aα-chains pass through the peripheral D regions, fold back to form a fourth alpha helix in the distal third of the coiled-coil and thereafter their structure is not resolved (1). This unresolved segment, or αC region, comprises about 65% of the Aα chain and about one fourth of the mass of the fibrinogen molecule.

The structure and function of the αC region has been the focus of many studies. As summarized in a decade-old review (3), this region (human Aα residues 221-610) can be described as two parts, the αC connector and the αC domain. Scanning micro-calorimetry experiments (4) and more recently NMR structure analysis (5) show the αC domain (Aα 392-610) is an independently folded compact structure. Within the fibrinogen molecule, the two αC domains appear to interact with one another and with the central E region (3, 6). During the conversion of soluble fibrinogen into fibrin fibers, the protease thrombin cleaves fibrinogen releasing two short fibrinopeptides, FpA and FpB, from the N-termini of the Aα and Bβ chains respectively. The release of FpA exposes the polymerization knobs called ‘A’ in the central E region of one molecule that bind to the polymerization holes called ‘a’ in the peripheral D regions in two other molecules. These ‘A:a’, knob:hole, interactions support formation of double-stranded, half-staggered linear polymers called protofibrils. Following the loss of FpB, the αC domains dissociate from the E region and become available for intermolecular interactions (7). Several experiments (3) suggest a model where such intermolecular interactions support the assembly of protofibrils into fibrin fibers; this assembly is usually called lateral aggregation.

Our previous studies have shown that engineered variant fibrinogens are useful tools to identify residues and domains that are critical to fibrinogen function. For example, fibrinogens with substitutions in hole ‘a’ show ‘A:a’ interactions are critical for protofibril formation while variants with substitutions in hole ‘b’ show ‘B:b’ interactions do not have a critical role in polymerization (8, 9). To examine the role of the αC domains, we synthesized a recombinant fibrinogen lacking residues 252-610, Aα251 fibrinogen. Studies with this variant have shown that the role of the αC domain in polymerization was less significant than was previously thought (10). Polymerization of Aα251 fibrinogen was similar to normal recombinant fibrinogen, although the Aα251 fibrin fibers were somewhat thinner than normal fibers (11). Most importantly, these studies showed that the αC domains are not required for lateral aggregation, as a stable fibrin clot was formed by Aα251 fibrinogen.

To resolve the apparent contradictions in the role of the αC region in polymerization, we synthesized a hybrid fibrinogen containing normal human fibrinogen chains, but substituting the chicken αC region for the human αC region. The chicken segment lacks the tandem repeats that are present in the human αC connector, but has homology to the human sequence near the disulfide-linked β-hairpin that centers the structured αC domain (12). Because the overall shape of chicken fibrinogen is not different from human, we expected the hybrid molecule would have the same shape as human fibrinogen (1, 13, 14) introducing this change, we altered the αC region while preserving the potential for normal chicken intra- and inter-molecular αC-αC interactions. Herein, we present data on the synthesis and expression of human/chicken hybrid (HC) fibrinogen, its structure and its polymerization. This variant apparently is the first to target lateral aggregation.

Experimental Procedures

Materials

All chemicals were of reagent grade and were purchased from Sigma-Aldrich (St. Louis, MO), unless specified otherwise. The peptide GPRP-amide was purchased from Bachem Americas, Inc. (Torrance, CA). Cell culture media with normal recombinant fibrinogen were obtained from the National Cell Culture Center (Biovest International, Minneapolis, MN). Monoclonal IF-1 antibody was purchased from Kamiya Biomedical (Seattle, WA). Human α-thrombin (HT 1002a) and human plasmin (HPlasmin) were from Enzyme Research Laboratories, Inc (South Bend, IN). Rabbit polyclonal antibodies to human fibrinogen were purchased from Dako Corp, code N A0080 (Carpinteria, CA). Monoclonal antibody Y18 (15) was a gift from Dr. Nieuwenhiuzen (Leiden, The Netherlands). A monoclonal antibody specific for the N-terminus of the Bβ chain (16) was provided by Dr. Shainoff (Cleveland State University, Cleveland, OH). Monoclonal antibody 4A5 (17) was a gift from Dr. Matsueda (Bristol-Myers Squibb, Princeton, NJ).

Synthesis of the human/chicken hybrid Aα chain

The cDNA encoding the human 19 residue signal sequence, human Aα residues 1-197 and chicken Aα residues 199-491 was synthesized and cloned into the expression vector p284 (18) by GenScript USA Inc. (Piscataway, NJ). The entire coding region of the plasmid was sequenced to ensure the appropriate polypeptide was encoded (UNC Automated DNA Sequencing Facility, Chapel Hill, North Carolina, USA). The mutant expression plasmid was co-transfected with pMLP-γ and the selection plasmid pMLVhis into Chinese Hamster Ovary cells containing the normal Bβ expression plasmid as described (18). The clone producing the highest level of fibrinogen, as determined by an enzyme-linked immunosorbent assay, was selected and grown in roller bottles in serum-free medium containing aprotinin. The culture medium was harvested periodically; after adding PMSF, the medium was stored at −20°C until fibrinogen purification. Normal recombinant fibrinogen was synthesized by similar methods as reported previously (19).

Fibrinogen purification

Fibrinogen was purified as described (8, 19) by immunoaffinity chromatography, using the calcium-dependent fibrinogen-specific monoclonal antibody IF-1. Briefly, fibrinogen was precipitated from the medium with ammonium sulfate; the pellet was dissolved in buffer with 10 mM $CaCl_2$ and loaded onto the IF-1 column. Bound fibrinogen was eluted using EDTA-containing buffer, dialyzed once against loading buffer and then extensively against 20 mM HEPES, pH 7.4, 150 mM NaCl (HBS) buffer.

SDS-PAGE and Western Blot

Reduced and non-reduced samples of both fibrinogens were separated on SDS polyacrylamide gels (10 and 8 %, respectively) and either stained with Coomassie Blue G-250 or transferred onto 0.45 μm nitrocellulose (Bio-Rad, Hercules, CA) for Western blotting. The blots were developed as described (19) with either an anti-fibrinogen polyclonal antibodies (Dako, Corp) or monoclonal antibody Y18, which recognizes the N terminus of the Aα chain of human fibrinogen (15), or a monoclonal antibody against residues 15-21 of the Bβ chain (16) or monoclonal antibody 4A5, which recognizes the C terminus of the γ chain (17). Bound antibodies were visualized by enhanced chemiluminescence (Amersham Pharmacia Biotech, Piscataway, NJ). Densitometry analysis of Y18 immunoblots was performed using ImageQuant software (GE Healthcare, Piscataway, NJ).

Fibrinopeptide release

The release of fibrinopeptides A and B was monitored by high-performance liquid chromatography (HPLC) as described (20, 21). Briefly, the reactions were initiated by adding thrombin (0.01 U/mL) to fibrinogen (0.1mg/mL) at time zero. The samples were mixed, aliquoted, and the reactions stopped at specific times by placing the samples in boiling water. Following centrifugation, the supernatants were injected onto a reversed-phase column (5μm C18, 4.6×24mm, Discovery, Supelco; Sigma-Aldrich) and analyzed by HPLC (Shimazdu) with an acetonitrile gradient. The areas under the peaks corresponding to FpA and FpB were measured, converted to percent fibrinopeptide released, and graphed using Origin (OriginLab, Northampton, MA). The data were fit to a first-order equation for FpA and to two sequential first-order equations for FpB. The specificity constants (kcat/Km) were calculated by dividing the rate constants by the thrombin concentration.

Polymerization measured by turbidity

Polymerization at ambient temperature was monitored by turbidity, essentially as described (22). Briefly, fibrinogens were dialyzed overnight at 4°C in HBS, and diluted to 1.2 μM in HBS with 1 mM $CaCl_2$. Fifty microliters fibrinogen was placed in a microtiter plate (Corning Costar, Corning, New York, USA) well, and the reaction was initiated by the addition of 50 μl of thrombin using a multichannel pipette. The final fibrinogen and thrombin concentrations were 0.6 μM and 0.1 U/mL, respectively. For normal fibrinogen the concentration was determined using the extinction coefficient at 280 nm of 1.51 for 1 mg/mL and 340,000 Da mass; for HC fibrinogen the concentration was determined using the extinction coefficient at 280 nm of 1.31 for 1 mg/mL and 314,270 Da mass. Polymerization was followed at 350 nm on a SpectraMax 340PC microplate reader (Molecular Devices, Sunnyvale, CA, USA). The turbidity curves were graphed using Origin (OriginLab, Northampton, MA).

Dynamic Light Scattering (DLS)

All measurements were performed at 25°C in the DynaPro™ Plate Reader™ from Wyatt Technology Corporation (Santa Barbara, CA). All the samples were filtered (0.22 μm GV DURAPORE centrifugal filter) prior to use. Measurements were monitored as the change of hydrodynamic radius, determined using the software provided with the instrument. The hydrodynamic radius of fibrinogen was determined in HBS before and after gel filtration chromatography. Polymerization was monitored by DLS following the rise in average hydrodynamic radius. Right before polymerization, human α-thrombin was diluted into filtered HBS with 1 mM $CaCl_2$ to 0.02 U/mL. Reactions were initiated by adding 60 μL of thrombin into a tube which contained 60 μL of fibrinogen (0.8 mg/mL in HBS with 1 mM $CaCl_2$), mixed well, and immediately transferred into the plate reader wells. Data was collected every 10 sec.

Gel filtration chromatography

Fibrinogen monomers were prepared by gel filtration chromatography using an FPLC system (Pharmacia Biotech, Piscataway, NJ). Fibrinogen samples (8-10 mg/mL in HBS) were injected onto a Superdex-200 (GE Healthcare, Piscataway, NJ) column equilibrated with HBS buffer. Fractions (120 μL/tube) were collected while monitoring elution at 280 nm. For each fraction the average hydrodynamic radius was determined by DLS and the protein concentration determined using the Nanodrop spectrometer (Nanodrop 2000, Thermo Scientific, Wilmington, DE). The peak fractions, which corresponded to fibrinogen monomers, were pooled, adjusted to 0.8 mg/mL in HBS with 1 mM $CaCl_2$, and stored at 4°C until use within 48 hrs.

Plasmin digests

Plasmin digests and the plasmin protection assay was performed as described (23). Briefly, fibrinogen (0.29 mg/mL for HC, 0.26 mg/mL for normal) was incubated with 10 μg/mL plasmin in HBS buffer with 5 mM $CaCl_2$ or 5 mM EDTA, with and without GPRP for 4 h at 37°C. The reactions were stopped by the addition of SDS-PAGE sample buffer, heated in a 100°C water bath for 15 min and analyzed by SDS-PAGE (8%) run under non-reducing conditions.

Peptide mass fingerprinting (PMF)

Samples for PMF were prepared by in-gel digestion of the two HC bands manually excised from a reduced SDS-PAGE separation on a 7.5% gel. Each polyacrylamide strip was digested essentially as described (24) with the exception that samples were incubated with trypsin (Trypsin Gold, Mass Spectrometry Grade; Promega; Madison, WI, USA) for 2 hours at 4°C and then overnight at 37°C. The digests were analyzed by reverse phase HPLC-electrospray ionization (RP-HPLC-ESI)/time of flight mass spectrometry (TOF MS) using a 6210 Time of Flight LC/MS (Agilent) coupled with an Agilent 1200 series HPLC system. Peptide separation was performed on a ZORBAX SB C18 column (Agilent Technologies) at a flow rate of 20 μl/ min at 30°C with the sequence: isocratic 2% B for 10 min, a linear gradient over the course of 50 min to 70% B, a linear gradient to 100% B in 5 min and finally maintained at 100% B for 15 min, where solvent B was 0.1% formic acid in acetonitrile, and solvent A was 0.1% formic acid in water. The peak list for the PMF analysis was created using the Agilent's MassHunter software. The search was done using the Spectrum Mill MS Proteomics Workbench (Agilent Technologies) software against the complete SwissProt database. The following parameters were used in the search: taxonomy, all species; protein molecular mass, 1000-150,000. The cleavage rule for trypsin was designated and the allowance for number of missed cleavages was set at 1. The peptide tolerance did not exceed 5 ppm. Carbamidomethylation was set as fixed modification while methionine oxidation as variable modification.

Results

Generation of human/chicken hybrid fibrinogen

The plasmid expression vector encoding a hybrid Aα chain and containing the N-terminus of the human and the C-terminus of the chicken Aα chains was constructed by gene synthesis as described in Experimental Procedures. The selection of the junction between the human and chicken sequences was based on sequence alignment and the crystal structures of the two fibrinogens. Our goal was to maintain all the structure that is seen in the human crystal and replace the human αC region with the chicken αC region. The hybrid cDNA encodes human residues Aα Ala1-Arg197 and chicken residues Aα Gln199 - Lys491 (Figure 1). Arg197 is 9 residues from the end of the fourth α-helix of the coiled-coil in human (1). Gln199 is 10 residues from the end of the fourth α-helix of the coiled-coil in chicken (13). Such composition preserves the human sequence throughout the coiled-coil and links the human sequence to the chicken sequence in a similar position.

Synthesis and characterization of human/chicken hybrid fibrinogen

The hybrid plasmid expression vector was transfected into CHO cells as described in Experimental Procedures. We identified several cell lines that expressed the hybrid protein in amounts similar to that found with normal human fibrinogen. The cell line with the highest expression was selected for large scale culture. Although expression varied from culture to culture, the highest concentrations of hybrid fibrinogen, ~5 mg/L, were comparable to the typical concentrations of normal recombinant fibrinogen, ~7 mg/L. These

data show the presence of chicken αC did not significantly impair synthesis and secretion from mammalian cells indicating that this domain is not critical for chain assembly and protein secretion.

The hybrid fibrinogen, which we call HC fibrinogen, was purified using the usual protocol for recombinant fibrinogen as described in Experimental Procedures. The pure protein was characterized by SDS-PAGE and immunoblots (Figure 2). SDS-PAGE under non-reducing conditions (Figure 2A) showed only two bands, one whose migration was consistent with the expected mass for the molecule diagramed in Figure 1A, ~315,000 Da, and one slightly smaller. Immunoblots with polyclonal anti-fibrinogen antibodies confirmed both bands are fibrinogen and both react with the monoclonal antibody Y18(15), which is specific for the N-terminus of the human Aα chain (data not shown). These data indicate the normal and hybrid chains were assembled into two proteins, the expected protein with two copies of each of the three encoded chains and a slightly smaller protein. Analysis of HC fibrinogen under reducing conditions (Figure 2B) showed two bands on SDS-PAGE, whose migrations are equivalent to the normal human Bβ and γ chains. Immunoblot analysis showed these bands reacted with monoclonal antibodies specific for the human Bβ and γ chains (Figure 2C). Immunoblots developed with the monoclonal antibody Y18 showed both bands reacted with approximately equal intensity (Figure 2C). These bands are consistent with the full length HC Aα chain (calculated mass 54,229) and a truncated HC Aα chain with mass similar to the human γ chain. Densitometry of Y18 immunoblots showed the larger Aα chain in HC fibrinogen contained 50-60% of all Y18 intensity. Considered together the results with the non-reduced and reduced gels indicate that both hybrid Aα chains were assembled into HC fibrinogen molecules. These molecules appear analogous to the well-described HMW and LMW fibrinogens found in human plasma, which differ because the smaller species has a degraded Aα chain. Here the different sizes seen under non-reducing conditions likely reflect the differences in the length of the HC hybrid Aα chains seen under reducing conditions.

We confirmed the identities of the bands seen under reducing conditions by peptide mass fingerprinting. Tryptic peptides from in-gel digestion of each band were analyzed by RP-HPLC-ESI/TOF MS. The data showed the higher mass band contained peptides from the human Bβ, the human Aα and the chicken Aα chains, and the lower mass band contained peptides from the human γ, the human Aα and the chicken Aα chains. (Supplementary Figure S1.) The identified human Aα chain peptides were nearly the same for both bands, accounting for 39% (higher mass band) and 42% (lower mass band) of the 197 encoded human residues. In contrast, peptides coverage for the 293 encoded chicken residues was different, 56% for the higher mass band and 46% for the lower mass band. The reduced coverage for the lower band was mainly due to the absence of any peptide after residue K433. A hybrid chain terminating at residue 433 would have a mass of 48.0 kDa, and could be expected to co-migrate on SDS-PAGE with the normal γ chain. Analysis of the higher mass band identified Aα chain peptides covering through chicken residue K468. The full length hybrid chain would have a mass of 54.2 kDa, while termination at K468 would give a mass of 51.8 kDa. Although either mass might be expected to co-migrate with the normal Bβ chain, the mass of the full-length hybrid chain is closer to the mass of the Bβ chain, 54.4 kDa.

We further characterized the HC fibrinogen structure using plasmin digests, including plasmin protection assays (23). As shown in Figure 3, these data were analogous to normal fibrinogen. Plasmin digests of HC fibrinogen in the presence of calcium produced two fragments similar to normal fragments D1 and E. For both fibrinogens the intensity of the larger fragment was higher than that of the smaller, reflecting the 2:1 stoichiometry of the D and E regions. In the presence of EDTA, plasmin cleavage of HC fibrinogen resulted in two

bands analogous to fragments D2 and D3 seen with normal fibrinogen. Addition of GPRP peptide in the presence of EDTA limited plasmin cleavage, producing only one fragment analogous to fragment D1 seen with normal fibrinogen. Plasmin digests in the presence of calcium with or without GPRP peptide also showed only one fragment, equivalent to D1. These data indicate that the hybrid chain did not change the overall trinodular structure of fibrinogen and that the D region in HC fibrinogen has the same overall structure as the D region in normal fibrinogen. In particular, calcium binding and the knob:hole interactions known as 'A:a' are fully preserved in the HC hybrid fibrinogen.

Fibrin polymerization

We followed the kinetics of thrombin-catalyzed fibrinopeptide release and found both the rates and the quantities of fibrinopeptides released from the HC fibrinogen were indistinguishable from normal. The specificity constants for FpA were $(7.0 \pm 2.6) \times 10^6$ $M^{-1}s^{-1}$ (average ± SD) for HC fibrinogen and $(6.5 \pm 2.1) \times 10^6$ $M^{-1}s^{-1}$ for normal (n=4; p =0.26); for FpB these were $(3.2 \pm 0.8) \times 10^6$ $M^{-1}s^{-1}$ for HC fibrinogen and $(3.6 \pm 1.0) \times 10^6$ $M^{-1}s^{-1}$ for normal (n=4; p=0.65). FpB is normally released from desA fibrin polymers (25). Thus, the normal rate of FpB release from HC fibrinogen indicates that desA HC fibrin forms polymers. Consistent with the formation of HC fibrin polymers, we observed a change in viscosity, from a liquid to a gel, following incubation of HC fibrinogen with thrombin.

We followed thrombin-catalyzed polymerization by turbidity as described in Experimental Procedures. As shown in Figure 4A and Table 1, polymerization of HC fibrinogen was markedly different from normal. Turbidity increased from the very beginning of the reaction, with no obvious lag period, and plateaued at 0.014 after about 15 min. Under the same conditions, normal fibrinogen had a lag period of 3.2 min, after which the turbidity increased rapidly to 0.185, reaching this plateau after about 20 min. As the fibrinopeptide release assays indicate FpA release is normal and the plasmin protection assays indicate 'A:a' interactions are normal, these turbidity data suggest that the hybrid Aα chains interfere with lateral aggregation.

In order to better visualize the differences, we followed polymerization by dynamic light scattering (DLS). These studies were performed with the DynaPro™ DLS Plate Reader, which enables real-time tracking of DLS from small volume samples. As described in Experimental Procedures, we mixed thrombin with fibrinogen, transferred the reaction mixtures to the plate reader, and followed the change in DLS at 25°C. DLS measures the diffusion coefficient of particles in the sample, which the DynaPro™ software converts to the hydrodynamic radius assuming the particles are spheres. Clearly, this assumption is not appropriate for the formation of fibrin fibers. Nevertheless, the DLS measurements show changes in "size" from monomers to oligomers, whether protofibrils or fibers. The first experiments showed that the normal and HC fibrinogens were not monodisperse; the average hydrodynamic radius indicated fibrinogen aggregates were present in both fibrinogens (Table 2). We purified fibrinogen monomers by gel filtration chromatography as described in Experimental Procedures. DLS measurements (Table 2) showed the purified proteins have an average hydrodynamic radius consistent with prior determinations for fibrinogen monomers (26): 9.7 nm for normal fibrinogen and 9.6 nm for HC fibrinogen. We followed polymerization of purified fibrinogen monomers by DLS (Figure 4B) using 0.4 mg/mL fibrinogen and 0.01 U/mL thrombin. Under these conditions, polymerization occurs more slowly than in the turbidity experiments. For normal fibrinogen, the DLS curve had a lag period with a relatively modest increase (see insert in Figure 4B) in the average hydrodynamic radius for 25 min followed by a rapid increase in hydrodynamic radius reaching a maximum around 40 min. In contrast, with HC fibrinogen there was only a modest increase in average hydrodynamic radius throughout the 70 min time course of the reaction (see insert in Figure 4B). Thus, HC monomers continued to assemble into larger

species but did not show the rapid increase associated with lateral aggregation. During the first 15-20 min of the reactions the rate of increase in hydrodynamic radius for HC fibrinogen was similar to the rate of increase for normal fibrinogen. This suggests that the HC fibrin monomers assemble into larger complexes in a manner similar to normal protofibril formation. If HC monomers indeed form structures analogous to protofibrils, then the low hydrodynamic radius for HC fibrin at 70 min indicates that lateral aggregation of such protofibrils is remarkably less efficient than normal or indeed does not occur.

Copolymerization of HC and normal fibrinogens

To determine whether HC and normal fibrinogens could form a copolymer, we mixed the fibrinogens prior to adding thrombin and followed polymerization by turbidity. The data, shown in Figure 5 and Table 1, indicate that copolymers are formed and that the HC fibrin dominates the polymerization of these copolymers. In these studies the total fibrinogen concentration was maintained at 0.6 μM. Adding as little as 10% (mole:mole) HC fibrinogen to normal fibrinogen noticeably changed polymerization, increasing the lag time, decreasing the slope of the rising turbidity and reducing the final absorbance relative to normal fibrinogen alone. Increasing the mole fraction of HC fibrinogen to 25% further increased the lag time, and further decreased the slope and the final absorbance. Polymerization of a 50:50 mixture of HC and normal fibrinogens looked the same as polymerization of pure HC fibrinogen, with a slow rise in turbidity, and a slowly decreasing slope until a plateau was reached after ~ 2 hours. These results demonstrate that the two fibrinogens interact with one another. For example, if the fibrinogens did not interact, one would expect the 50:50 mixture to have a final absorbance between the final absorbance for normal (0.185) and the final absorbance for HC (0.014). As the final absorbance with the 50:50 mixture was the same as that with pure HC fibrinogen, the HC fibrin interacted with normal fibrin in a way that inhibited the polymerization of the normal fibrin in the mixture. The curves seen in mixtures with 10% or 25% HC fibrinogen showed a pattern similar to normal fibrinogen, a rapid increase in turbidity followed by a plateau. The shape of these curves suggests that the two fibrinogens assemble together into fibers.

We also examined polymerization of mixtures using DLS. The data (Figure 6A, B) were analogous to the turbidity data. With equimolar amounts of HC and normal fibrinogens, the DLS profile was indistinguishable from pure HC fibrinogen. The mix with 25% HC fibrinogen showed an increased lag time and a lower final radius than normal fibrinogen, again clearly different from the profile expected for the sum of the two pure proteins. As shown in Figure 6B, the rate of increase in hydrodynamic radius during the lag time was essentially the same for all samples. Based on these data we conclude that the assembly of fibrin monomers into larger species proceeds at the same rate, whether the monomers are normal, HC, or a mixture of normal and HC fibrins. The common slope seen for all samples suggests that protofibrils or protofibril-like structures are formed in all cases. For normal fibrinogen the increase in hydrodynamic radius during the lag time represents an increase in the size of protofibrils and a decrease in the number of monomers. Because the slope of profile obtained with pure HC and the 50:50 mixture decreases with time, it is reasonable to conclude that this profile represents only an increase in the size of protofibrils and a decrease in the number of monomers. The rate of protofibril assembly slows as the concentration of monomers becomes limiting, and eventually the curve reaches a plateau. Of course, it is possible that this profile represents the slow assembly of protofibrils into very thin fibers, or the assembly into oligomers that are not like protofibrils. In any case, the profile clearly demonstrates that oligomers of HC monomers or equimolar mixture of HC and normal monomers do not assemble into fibers at the accelerated rate seen with normal fibrinogen.

Turbidity profiles with fibrinogen monomers

Fibrin polymerization is a kinetically controlled process (27). Therefore, the presence of even a small number of aggregates (oligomers) in our fibrinogen preparations (as we detected by DLS, Table 2) could alter polymerization. To examine this possibility, we repeated some turbidity experiments using the monomeric fibrinogens purified by gel-filtration chromatography. Representative data are shown in Figure 6C. The turbidity profiles were slightly different from those obtained prior to purification. Nevertheless, the profile for the 50:50 mixture was still indistinguishable from that for pure HC fibrinogen, and the 25:75 mixture still had a longer lag time, and a decreased slope and final absorbance relative to the pure normal fibrinogen. It is notable that both turbidity profiles had a higher final absorbance than the comparable profiles obtained prior to gel filtration purification (Compare normal and 25:75 mixtures in Figure 5 to Figure 6). As shown in Figure 6D, the profiles of all samples were indistinguishable during the lag times, consistent with our conclusion that the assembly of fibrin monomers into larger complexes proceeds at the same rate, whether the monomers are normal, HC, or a mixture of normal and HC fibrins.

We also compared the turbidity profile of the 25:75 mixture to profiles obtained with reduced concentrations of normal fibrinogen monomers, 0.45 μM and 0.3 μM, or 75% and 50% of the concentration in the copolymerization experiments (Figure 7). The turbidity profile of normal monomeric fibrinogen at 0.3 μM (50% concentration) was most similar to that of the copolymerization profile with the 25:75 mixture. The lag time for polymerization with 25% HC fibrinogen was ~1.5 fold longer, the maximum slope about the same, and the final A350 slightly increased relative to normal fibrinogen at 0.3 μM. Comparing the profile with 25:75 mixture to the profile at 75% concentration of normal fibrinogen (0.45 μM), it is clear that the presence of HC fibrinogen markedly altered polymerization. We conclude that the formation of copolymers of normal and HC fibrinogens was not dependent on the complexes that were present in these fibrinogens before gel-filtration. Copolymers were formed between chromatography-purified monomers and the turbidity profiles were dominated by the HC fibrinogen.

Discussion

Our data show the substitution of the human αC region by the homologous chicken αC region did not alter the early steps in polymerization. Thrombin-catalyzed release of both FpA and FpB was indistinguishable from normal. The normal rate of FpB release indicates not only normal interactions between HC fibrinogen and human thrombin, but also normal initiation of protofibril formation. Studies with variants that alter ‘A:a’ interactions have shown that a delay in the association of monomers into protofibrils is reflected in a delay of FpB release (28). Further, previous electron microscopy studies have shown that the normal αC domain interacts with the central domain and that the release of FpB correlates with the loss of this interaction (29). Thus, the normal rate of FpB release suggests normal ‘A:a’ interactions, normal assembly of desA fibrin monomers, and no clash between the chicken αC and the central domain structures that are critical for thrombin binding and fibrinopeptide release. Consistent with these findings, the plasmin protection assays showed normal GPRP peptide binding suggesting normal ‘A:a’ interactions.

In contrast, the turbidity and DLS data show the chicken segment markedly altered polymerization. We analyzed the data as if all species of HC fibrinogen contributed to the results, which may not be correct. Nevertheless, even if only one species is reactive, this species has a profound impact on polymerization. Our data show HC monomers assemble into oligomers in a time-dependent manner. These data are consistent with the conclusion that only protofibrils, or very thin fibers, are formed when the chicken segment is present in fibrinogen. Because the same initial increase in DLS was seen in all polymerization curves,

with both mixed and unmixed proteins, it is reasonable to conclude that HC fibrin monomers assemble into half-staggered, double-stranded protofibrils or protofibril like structures. Both HC fibrinogen alone and the 50:50 mixtures show no steep rise in turbidity, but rather continue to increase with a slowly decreasing slope until a plateau is reached after ~ 2 hours. This gradual change in slope suggests that the concentration of protofibrils increases with time until all (or most) fibrin monomers are incorporated into protofibrils. We conclude that the shape of these curves is consistent with the formation of only protofibrils. Further studies using different approaches are needed to determine whether or not half-staggered, double-stranded protofibrils are formed and whether these are assembled into thin fibers.

Analysis of polymerization with purified fibrinogen monomers showed only the shape of the curve early in either turbidity or DLS is altered when larger species, probably fibrinogen aggregates, are removed from the sample. Removing these aggregates changed the kinetics but did not alter the markedly lower final turbidity or final hydrodynamic radius seen with HC fibrinogen. We conclude that the presence of aggregates altered the kinetics of protofibril formation for both fibrinogens, but did not influence the functional differences between HC and normal fibrinogen.

The increase in lag time seen in the copolymerization of HC and normal fibrinogens suggests that the altered Aα chains interfere with lateral aggregation. If the curves for HC alone represent an indefinite lag time with either no lateral aggregation or a delay in lateral aggregation beyond the time of this experiment (2 hrs, Figure 6B), then the addition of HC fibrinogen to normal fibrinogen would increase the lag time and impede lateral aggregation. On the other hand, if the polymerization curves for HC alone represent a short, immeasurable lag time, and immediate but impaired lateral aggregation with a low final turbidity and hydrodynamic radius, then one would expect addition of HC fibrinogen to normal fibrinogen would impede lateral aggregation but have no influence on the normal lag time. As reported here, an increase in the fraction of HC fibrinogen was associated with an increase in the lag time, from 3.1 min, to 3.4 min, to 5.3 min, to indefinite with 0%, 10%, 25% and 50% HC fibrinogen, respectively. We conclude that the chicken αC region impedes lateral aggregation, but not protofibril formation.

The rate of assembly of protofibrils into fibers and the final fiber diameter, reflected in the turbidity at 60 min, decreased with the fraction of HC fibrinogen, indicating that protofibrils containing the HC monomers were able to co-assemble along with protofibrils containing normal monomers. Nevertheless, this assembly process was impaired. With 25% HC the slope and the turbidity at 60 min were similar to normal fibrinogen at half the concentration in the fibrinogen mixture. This finding suggests the following model (Figure 8). Early in polymerization the normal and HC monomers assemble together at random, so every protofibril is a 25:75 mixture of HC and normal monomers. Lateral aggregation of these mixed protofibrils is impeded, as evidenced by the longer lag time. During this time, the association/dissociation equilibrium between monomers and protofibrils (25) allows a stochastic change in the relative contribution of HC monomers as well as the juxtaposition of normal and HC of monomers. Only the protofibrils that have a sufficient number of lateral aggregation sites exposed in the proper orientation will be able to laterally aggregate. The number and exposure of lateral aggregation sites is controlled by the number of normal fibrin monomers composing the protofibril. Whenever protofibrils form where the composition and/or sequence of normal monomers allows for lateral aggregation, these protofibrils will assemble rapidly into fibers. Such fibers are stable, so these monomers are removed from the reaction equilibrium. Assuming that the protofibrils that can assemble into fibers have more normal than HC monomers (i.e. less than 1 in 4 is HC monomer), the formation of fibers will lead to an increase in the representation of HC monomers in the monomer↔protofibril equilibrium. As a consequence, the relative concentration of HC

monomers and protofibrils containing more than 25% HC molecules increases throughout the reaction. As the reaction proceeds, the assembly of fibers will approach that seen in the 50:50 mixture. Undoubtedly other models are consistent with these data. Of particular relevance here, turbidity and light scattering measure bulk properties and cannot distinguish between a homogeneous sample with abnormal fibers and a heterogeneous sample with normal fibers and abnormal protofibrils.

In summary, our studies show HC fibrinogen is synthesized at normal levels and has the normal overall structure of human fibrinogen. Polymerization of this altered protein is abnormal, consistent with prior studies that show the αC domain has an important role in polymerization. The HC monomers can assemble into polymers; DLS data suggest these polymers are similar to normal protofibrils. Most significantly, these polymers cannot assemble fibrin fibers. That is, lateral aggregation either is not possible or is extremely impaired. Further studies, including electron microscopy, are in progress to compare normal human, normal chicken, HC and Aα251 fibrinogens. We anticipate these studies will provide insight into the molecular processes that regulate lateral aggregation.

Supplementary Material

Refer to Web version on PubMed Central for supplementary material.

Acknowledgments

We thank Brian Holliday (Chapel Hill, NC, USA) for technical assistance, Dr. Mattia Rocco and Anna Aprile (Genoa, Italy) for assistance with the mass spectrometry sample preparations and analysis, Dr. Alisa S. Wolberg for her critical comments on the manuscript and the Macromolecular Interactions Facility (UNC-Chapel Hill) for use of the DynaPro™ Plate Reader™.

Abbreviations

HC	human-chicken hybrid
FpA	fibrinopeptide A
FpB	fibrinopeptide B
GPRP	Gly-Pro-Arg-Pro amide
HPLC	high performance liquid chromatography
FPLC	fast protein liquid chromatography
DLS	dynamic light scattering
HBS	20 mM HEPES, pH 7.4, 150 mM NaCl
SDS-PAGE	sodium dodecyl sulfate polyacrylamide gel electrophoresis

References

1. Kollman JM, Pandi L, Sawaya MR, Riley M, Doolittle RF. Crystal Structure of Human Fibrinogen. Biochemistry. 2009; 48:3877–3886. [PubMed: 19296670]
2. Medved L, Weisel JW. Recommendations for nomenclature on fibrinogen and fibrin. J Thromb Haemost. 2009; 7:355–359. [PubMed: 19036059]
3. Weisel JW, Medved L. The structure and function of the alpha C domains of fibrinogen. Ann N Y Acad Sci. 2001; 936:312–327. [PubMed: 11460487]
4. Medved LV, Gorkun OV, Privalov PL. Structural organization of C-terminal parts of fibrinogen A alpha-chains. FEBS Letters. 1983; 160:291–295. [PubMed: 6224704]

5. Tsurupa G, Hantgan RR, Burton RA, Pechik I, Tjandra N, Medved L. Structure, Stability, and Interaction of the Fibrin(ogen) Î±C-Domains. Biochemistry. 2009; 48:12191–12201. [PubMed: 19928926]
6. Litvinov RI, Yakovlev S, Tsurupa G, Gorkun OV, Medved L, Weisel JW. Direct Evidence for Specific Interactions of the Fibrinogen aC-Domains with the Central E Region and with Each Other. Biochemistry. 2007; 46:9133–9142. [PubMed: 17630702]
7. Gorkun OV, Veklich YI, Medved LV, Henschen AH, Weisel JW. Role of the alpha C domains of fibrin in clot formation. Biochemistry. 1994; 33:6986–6997. [PubMed: 8204632]
8. Okumura N, Gorkun OV, Lord ST. Severely impaired polymerization of recombinant fibrinogen gamma-364 Asp --> His, the substitution discovered in a heterozygous individual. J Biol Chem. 1997; 272:29596–29601. [PubMed: 9368024]
9. Bowley SR, Lord ST. Fibrinogen variant BbetaD432A has normal polymerization but does not bind knob “B”. Blood. 2009; 113:4425–4430. [PubMed: 19075185]
10. Gorkun OV, Henschen-Edman AH, Ping LF, Lord ST. Analysis of Aa251 fibrinogen: The aC domain has a role in polymerization, albeit more subtle than anticipated from the analogous proteolytic fragment X. Biochemistry. 1998; 37:15434–15441. [PubMed: 9799505]
11. Collet JP, Moen JL, Veklich YI, Gorkun OV, Lord ST, Montalescot G, Weisel JW. The alphaC domains of fibrinogen affect the structure of the fibrin clot, its physical properties, and its susceptibility to fibrinolysis. Blood. 2005; 106:3824–3830. [PubMed: 16091450]
12. Weissbach L, Grieninger G. Bipartite mRNA for chicken alpha-fibrinogen potentially encodes an amino acid sequence homologous to beta- and gamma-fibrinogens. Proc Natl Acad Sci USA. 1990; 87:5198–5202. [PubMed: 2367530]
13. Yang Z, Kollman JM, Pandi L, Doolittle RF. Crystal structure of native chicken fibrinogen at 2.7 A resolution. Biochemistry. 2001; 40:12515–12523. [PubMed: 11601975]
14. Cardinali B, Profumo A, Aprile A, Byron O, Morris G, Harding SE, Stafford WF, Rocco M. Hydrodynamic and mass spectrometry analysis of nearly-intact human fibrinogen, chicken fibrinogen, and of a substantially monodisperse human fibrinogen fragment X. Arch Biochem Biophys. 2010; 493:157–168. [PubMed: 19853574]
15. Koppert PW, Huijsmans CM, Nieuwenhuizen W. A monoclonal antibody, specific for human fibrinogen, fibrinopeptide A-containing fragments and not reacting with free fibrinopeptide A. Blood. 1985; 66:503–507. [PubMed: 4040783]
16. Valenzuela R, Shainoff JR, DiBello PM, Urbanic DA, Anderson JM, Matsueda GR, Kudryk BJ. Immunoelectrophoretic and immunohistochemical characterizations of fibrinogen derivatives in atherosclerotic aortic intimas and vascular prosthesis pseudo-intimas. Am J Path. 1992; 141:861–880. [PubMed: 1415480]
17. Shiba E, Lindon JN, Kushner L, Matsueda GR, Hawiger J, Kloczewiak M, Kudryk B, Salzman EW. Antibody-detectable changes in fibrinogen adsorption affecting platelet activation on polymer surfaces. Am J Physiol. 1991; 260:C965–974. [PubMed: 2035620]
18. Binnie CG, Hettasch JM, Strickland E, Lord ST. Characterization of purified recombinant fibrinogen: partial phosphorylation of fibrinopeptide A. Biochemistry. 1993; 32:107–113. [PubMed: 8418831]
19. Gorkun OV, Veklich YI, Weisel JW, Lord ST. The conversion of fibrinogen to fibrin: recombinant fibrinogen typifies plasma fibrinogen. Blood. 1997; 89:4407–4414. [PubMed: 9192765]
20. Lord ST, Strickland E, Jayjock E. Strategy for recombinant multichain protein synthesis: fibrinogen B beta-chain variants as thrombin substrates. Biochemistry. 1996; 35:2342–2348. [PubMed: 8652575]
21. Mullin JL, Gorkun OV, Binnie CG, Lord ST. Recombinant fibrinogen studies reveal that thrombin specificity dictates order of fibrinopeptide release. J Biol Chem. 2000; 275:25239–25246. [PubMed: 10837485]
22. Mullin JL, Gorkun OV, Lord ST. Decreased lateral aggregation of a variant recombinant fibrinogen provides insight into the polymerization mechanism. Biochemistry. 2000; 39:9843–9849. [PubMed: 10933802]

23. Lounes KC, Ping L, Gorkun OV, Lord ST. Analysis of engineered fibrinogen variants suggests that an additional site mediates platelet aggregation and that “B-b” interactions have a role in protofibril formation. Biochemistry. 2002; 41:5291–5299. [PubMed: 11955079]

24. Shevchenko A, Wilm M, Vorm O, Mann M. Mass spectrometric sequencing of proteins silver-stained polyacrylamide gels. Anal Chem. 1996; 68:850–858. [PubMed: 8779443]

25. Lewis SD, Shields PP, Shafer JA. Characterization of the kinetic pathway for liberation of fibrinopeptides during assembly of fibrin. J Biol Chem. 1985; 260:10192–10199. [PubMed: 4019507]

26. Armstrong JK, Wenby RB, Meiselman HJ, Fisher TC. The hydrodynamic radii of macromolecules and their effect on red blood cell aggregation. Biophys J. 2004; 87:4259–4270. [PubMed: 15361408]

27. Weisel JW, Nagaswami C. Computer modeling of fibrin polymerization kinetics correlated with electron microscope and turbidity observations: clot structure and assembly are kinetically controlled. Biophys J. 1992; 63:111–128. [PubMed: 1420861]

28. Okumura N, Terasawa F, Haneishi A, Fujihara N, Hirota-Kawadobora M, Yamauchi K, Ota H, Lord ST. B:b interactions are essential for polymerization of variant fibrinogens with impaired holes ‘a’. J Thromb Haemost. 2007; 5:2352–2359. [PubMed: 17922804]

29. Veklich YI, Gorkun OV, Medved LV, Nieuwenhuizen W, Weisel JW. Carboxyl-terminal portions of the alpha chains of fibrinogen and fibrin. Localization by electron microscopy and the effects of isolated alpha C fragments on polymerization. J Biol Chem. 1993; 268:13577–13585. [PubMed: 8514790]

Figure 1.

Schematic of the junction of human and chicken Aα chain sequences. A segment of the human sequence (top line) is aligned with the similar segment of the chicken sequence (bottom line). Identical and similar residues are shaded. The human/chicken hybrid sequence includes human residues Ala1 through Arg197 joined to chicken residues Gln199 through Lys491. The encoded segment is shown in **BOLD**.

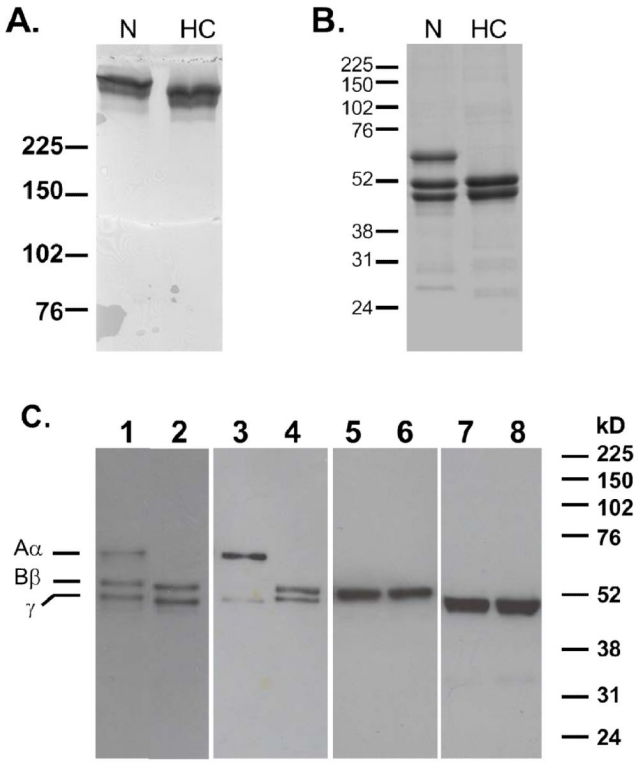

Figure 2.

SDS-PAGE and immunoblot analysis of human/chicken fibrinogen. Fibrinogens were analyzed by SDS-PAGE run under non-reducing (8% polyacrylamide, A) and reducing (10% polyacrylamide, B) conditions, and stained with Coomassie blue. Immunoblots (C) were prepared from 10% gels run under reducing conditions. Blots were developed with: a polyclonal antibodies to human fibrinogen (lanes 1 and 2); a monoclonal antibody specific for the N-terminus of the Aα chain (Lanes 3 and 4); a monoclonal antibody specific for the N-terminus of the Bβ chain (lanes 5 and 6); and a monoclonal antibody specific for the C-terminus of the γ chain (lanes 7 and 8). For all figures, odd numbered lanes are normal fibrinogen and even numbered lanes are HC fibrinogen. Molecular weight markers are indicated at the left (A and B) and on the right (C).

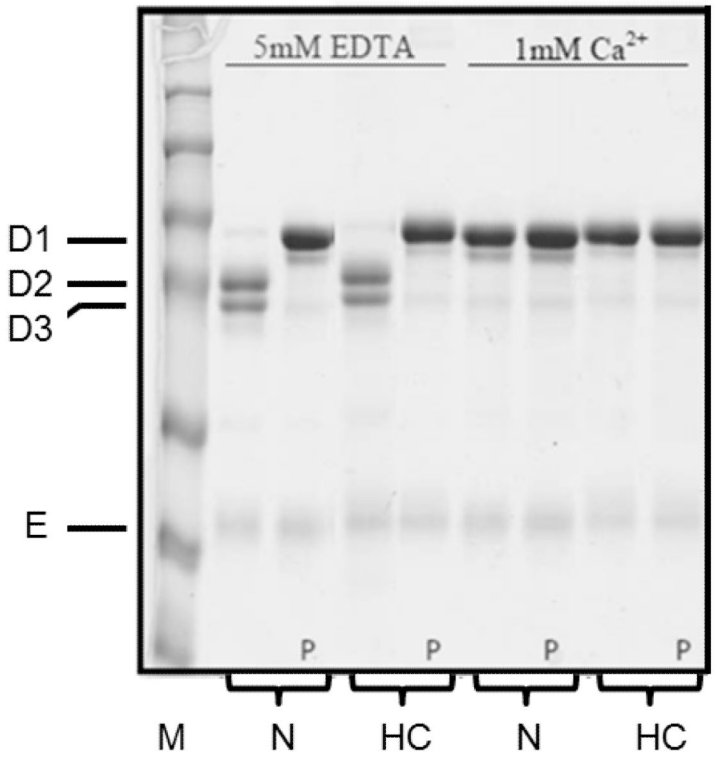

Figure 3.

Plasmin digests. Normal (N) and human-chicken (HC) fibrinogens with and without peptide GPRP (P) were incubated with plasmin in the presence of 5 mM EDTA or 1 mM $CaCl_2$. Samples were analyzed by SDS-PAGE (8%) run under non-reducing conditions. Normal plasmin digestion products D1, D2, D3 and E are indicated on the left.

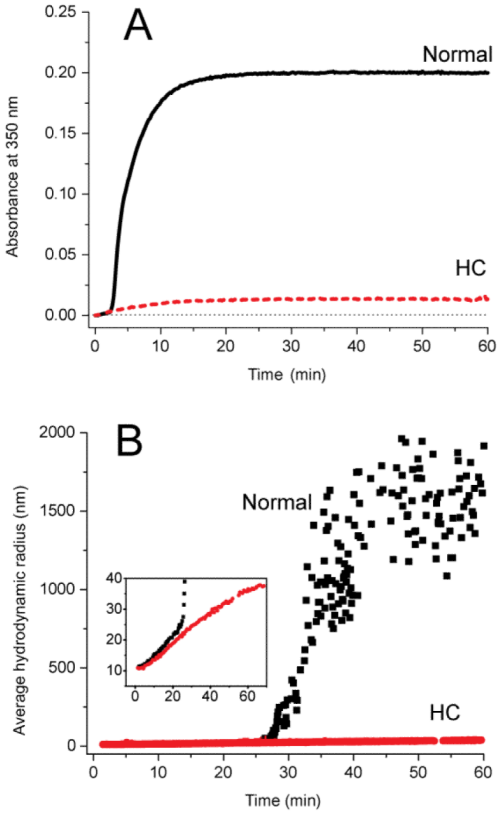

Figure 4.

Polymerization measured by turbidity (A) and dynamic light scattering (B). Polymerization was initiated by addition of thrombin to normal (solid line, solid squares) and HC (broken line, solid circles) fibrinogens. Representative turbidity curves (A) were obtained with 0.6 μM fibrinogen and 0.1 U/mL thrombin. The dotted line represents zero absorbance. Representative DLS curves (B) were obtained with 1.2 μM fibrinogen and 0.01 U/mL thrombin. The insert shows the same DLS data but on the different Y-scale.

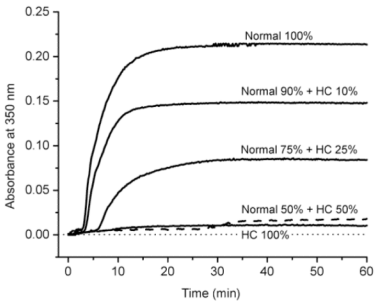

Figure 5.

Polymerization of fibrinogen mixtures. Polymerization was initiated by adding thrombin (0.1 U/mL) to normal or HC fibrinogens (0.6 μM) or their mixtures (mole/mole, 0.6 μM total fibrinogen). Polymer formation was measured by the change in turbidity with time. Representative curves (solid lines for all except the 50/50% N/HC mixture, broken line) from one experiment are shown. The dotted line represents zero absorbance.

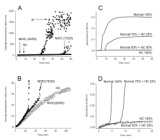

Figure 6.

Polymerization of fibrinogen monomers. Fibrinogen monomers were purified by gel-filtration chromatography. Representative results for thrombin-catalyzed (0.1 U/mL) polymerization of normal (N), HC and their mixtures (N/HC, percent of mole/mole). A representative polymerization experiment followed by DLS is shown in panels A and B. The presentation in panel B expands the Y-axis to show the time dependent change in radius for the relatively small forms, and extends the X-axis to show the gradually decreasing slope of the time-dependent change in radius for 100% HC (open circles) and the 50/50 normal/HC mixture (open triangles). A representative experiment followed by turbidity is shown in C and D. The presentation in panel D expands both axes to show the time dependent change at low turbidity at early times during polymerization. Both experiments were performed under conditions described in Figure 4.

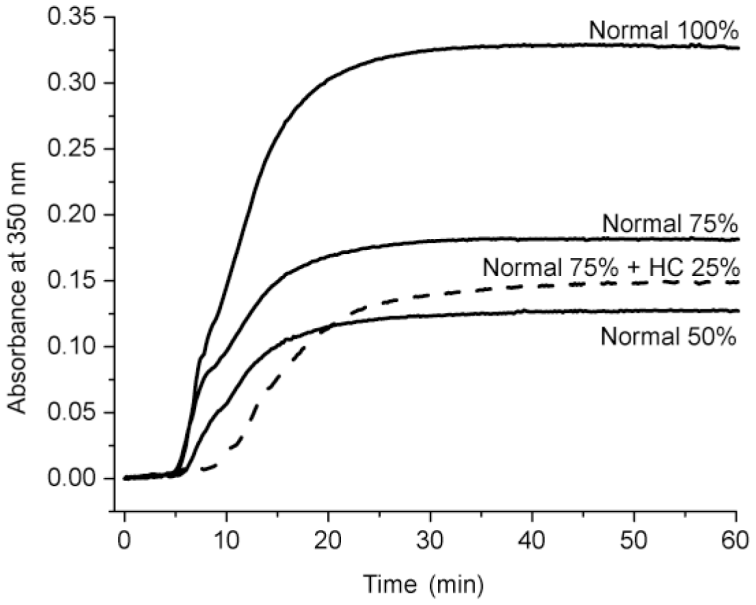

Figure 7.
Polymerization of the normal/HC mixture relative to normal fibrinogen. Polymerization of normal fibrinogen (solid lines) at 0.60 μM (100%), 0.45 μM (75%), and 0.30 μM (50%) and the 75:25 mixture (broken line) of 0.45 μM normal and 0.15 μM HC fibrinogens. Conditions were as described in Figure 4.

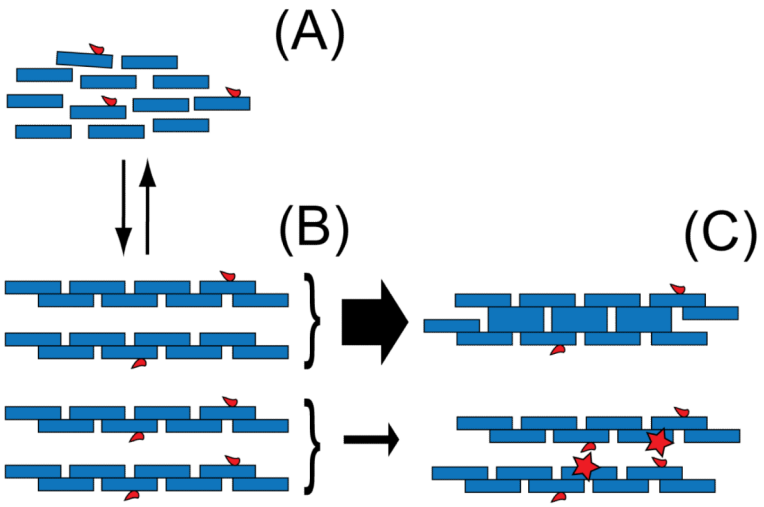

Figure 8.

Schematic of the model for polymerization of the 25:75 mixture of normal and HC fibrinogens. Normal fibrinogen is represented by a blue rectangle, HC by a blue rectangle with a red drop. Initially, the normal and HC monomers (A) assemble stochastically into mixed protofibrils (B). These protofibrils are in equilibrium with the monomers. The assembly of fibers (C) is rapid and irreversible (fat arrow) for protofibrils that are able to form fibers and slow (thin arrow) for protofibrils that are incapable of lateral aggregation. Red stars represent clashes between protofibrils that prevent or impair lateral aggregation. Assuming that the protofibrils that can assemble into fibers have more normal monomers (i.e. less than 1 in 4 is HC monomer), the formation of fibers will lead to an increase in the representation of HC monomers in the monomer↔protofibril equilibrium. As the reaction proceeds, the assembly of fibers will approach that seen in the 50:50 mixture. Thus, we expect the final clot will be a mixture of fibers, ranging from those found with normal fibrinogen at 0.3 μM to those found with the 50:50 mixture.

Table 1

Polymerization parameters calculated from the turbidity curves (mean ± SD).

Fibrinogen(s)	Lag-period (sec)	Maximum slope ($\times 10^{-5}$ s^{-1})	Final absorbance at 60 min
Normal	188±10	29±12	0.185±0.036
Normal + HC (90/10)	206±20	20±3	0.139±0.009
Normal + HC (75/25)	315±31	7±1	0.067±0.015
Normal + HC (50/50)	n/a	0.9±0.5	0.014±0.007
*Normal + HBS (50/50)	229±12	10±3	0.060±0.003
HC	n/a	0.7±0.5	0.014±0.003

* Polymerization of normal fibrinogen at half concentration (fibrinogen was diluted 50/50, v/v with HBS)

Table 2

Average hydrodynamic radius before and after gel-filtration chromatography purification. (Mean ± SD)

	Hydrodynamic radius (nm)	
	Before purification	**After purification**
Normal	17.8±0.2	9.7±0.1
HC	26.5±0.5	9.6±0.1